Int. J. Solids Structures Vol. 28, No. 5, pp. 549–565, 1991
Printed in Great Britain.

0020–7683/91 $3.00 + .00

BOUNDARY ELEMENT METHODS FOR THREE-DIMENSIONAL THERMOPLASTICITY

G. F. DARGUSH and P. K. BANERJEE
Department of Civil Engineering, State University of New York at Buffalo, Amherst, NY 14260, U.S.A.

(*Received* 8 *May* 1990; *in revised form* 30 *September* 1990)

Abstract—A new boundary element formulation is presented for quasistatic thermoplasticity. The governing integral equations utilize kernel functions based upon the fundamental solutions of uncoupled thermoelasticity, thereby eliminating volume discretization except in regions where plasticity occurs. As a result, the boundary element approach becomes an attractive alternative to finite element methods, particularly for problems involving localized plastic effects. In addition, the present work introduces a temperature-dependent strain-hardening material model and includes the body heat sources due to inelastic dissipation. The entire three-dimensional formulation has been implemented in a general-purpose boundary element code. Details of this numerical implementation are provided, along with results of several illustrative examples.

1. INTRODUCTION

In two previous papers (Dargush and Banerjee, 1989, 1990), boundary element methods (BEMs) were developed for linear problems of quasistatic thermoelasticity. However, contrary to common belief, the method is also well suited for nonlinear analyses. For example, the application of BEMs to time-independent plasticity is now standard textbook information (e.g. Banerjee and Butterfield, 1981), and, in some cases, significant computational advantages can be realized when compared with finite elements. This is particularly true if the plastic region represents only a small portion of the total body. A number of recent publications (Banerjee and Raveendra, 1986; Banerjee *et al.*, 1988, 1989) provide the framework for advanced elastoplastic BEM analysis.

In the present work, the boundary element method will be extended to thermoplasticity, including the effects of inelastic dissipation and a temperature-dependent yield surface. The first step in this process will be the derivation of a simple, yet meaningful, thermoplastic constitutive model in Section 2. Then, the integral formulation for generalized displacement rates and stress rates is developed in Section 3, based upon an initial stress approach. Armed with these relationships, Section 4 details the numerical implementation. Included is a description of the iterative time-marching process. However, to avoid unwarranted repetition, only those portions of the implementation that deviate from the linear algorithms (published earlier by Dargush and Banerjee, 1989, 1990) are discussed.

Before proceeding, it should be noted that this extension to thermoplasticity represents the very first BEM attempt at this class of problems. Much additional effort is required to transform this into a practical engineering analysis tool.

2. THERMOPLASTIC CONSTITUTIVE EQUATIONS

Before deriving the boundary integral formulation for nonlinear quasistatic thermal problems, a suitable material model is developed in this section. This new thermoplastic model is primarily intended for demonstrative purposes, and consequently has not been tailored to any specific material. However, as a first approximation, the model is appropriate for the analysis of a wide range of engineering materials. In particular, the following characteristics are included:

—time-independent behavior,
—temperature-dependent von Mises yield criterion,
—associative plastic flow,

—temperature-dependent isotropic hardening.
—elastic unloading during either a reduction in equivalent stress at constant temperature or a reduction in temperature at constant equivalent stress.
—recovery of temperature-independent elastoplastic behavior under isothermal conditions.

The model is based upon a straightforward extension of classical plasticity, thus retaining a formulation that requires only a minimal number of material parameters. It should be noted that certain portions of the development presented below have been extracted from Boley and Weiner (1960), where a temperature-dependent elastic–perfectly-plastic model is constructed. Other concepts have been borrowed from the Modified Cam Clay models (Roscoe and Burland, 1968) of soil plasticity and, in a sense, can be considered as an extension of the classical thermoelastic–poroelastic analogy.

As mentioned above, a temperature-dependent von Mises yield function is employed:

$$f(\sigma_{ij}, \theta, \varepsilon_{ij}^{p}) = J_2 - \frac{\sigma_y^2}{3}\Gamma \tag{1}$$

where J_2 is the second invariant of the deviatoric stress tensor, σ_y is the material yield strength in uniaxial tension at a reference temperature θ_{ref}, and Γ is a non-dimensional parameter that embodies the temperature dependence. Thus,

$$J_2 = \tfrac{1}{2}s_{ij}s_{ij}, \tag{2}$$

in which the deviatoric stress is given by

$$s_{ij} = \sigma_{ij} - \tfrac{1}{3}\delta_{ij}\sigma_{kk}. \tag{3}$$

Meanwhile, Γ is assumed to take the convenient, yet realistic, form

$$\Gamma = 1 - \left(\frac{\theta - \theta_{ref}}{\theta_{melt} - \theta_{ref}}\right)^2 \tag{4}$$

where θ_{melt} represents the melting temperature on an absolute scale. Additionally, the term σ_y acquires the value of the reference temperature yield strength associated with the current level of plastic strain.

This yield function is graphically portrayed on a $(J_2)^{1/2}$–$\beta\theta$ stress space plot in Fig. 1.

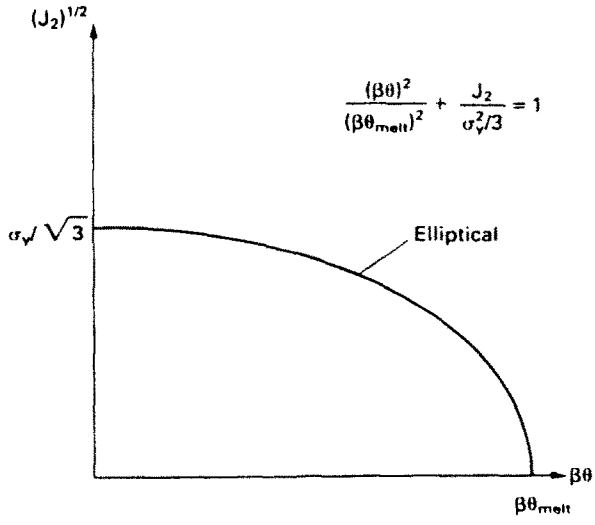

Fig. 1. Yield function in stress space ($\theta_{ref} = 0$).

where β is the material constant defined by

$$\beta = (3\lambda + 2\mu)\alpha = 3K\alpha, \tag{5}$$

with K representing the bulk modulus. Typically, in isothermal metal plasticity, yielding is related to the distortional components of deformation only. That is, dilatation is assumed to have no effect on yield strength. However, Fig. 1 clearly indicates that for the thermoplastic model the thermal portion of dilatational deformation does indeed have an impact on yield strength. Thus, even though the stress field is due exclusively to the mechanical strain, the magnitude of the thermal strain still contributes to the determination of the inception of yielding. In this regard, some parallels can be drawn to soil plasticity. For example, the diagram in Fig. 1 strongly resembles the elliptical $q-p$ relations used for Modified Cam Clay models, in which q is related to $(J_2)^{1/2}$ and p equals one-third of the first invariant of the effective stress tensor. For this clay model, the quantity p and, consequently, the yielding are dependent upon total dilatational deformation. Therefore, in both thermal and soil mechanics, the phenomenon of yielding is influenced by dilatational as well as distortional components of the deformation, although, typically, in thermomechanics only the temperature-induced portion of the dilatation is significant.

The next required ingredient is a plastic flow rule. The associated flow rule or normality condition relates the plastic strain rate to the normal of the yield surface in stress space:

$$\dot{\varepsilon}_{ij}^{p} = \dot{\lambda}\frac{\partial f}{\partial \sigma_{ij}}. \tag{6}$$

Finally, a work-hardening rule is needed. To maintain simplicity, an isotropic hardening model is selected. Figure 2 presents this expansion of the yield surface versus accumulated plastic strain in $(J_2)^{1/2}$–$\beta\theta$ space. It should be noted that while isotropic hardening is suitable for a first approximation, the model thus cannot predict many complex thermomechanical behaviors.

Expressing f as a function of stress, temperature and plastic strain permits the consistency condition to be written as

$$\mathrm{d}f = \frac{\partial f}{\partial \sigma_{ij}}\dot{\sigma}_{ij} + \frac{\partial f}{\partial \theta}\dot{\theta} + \frac{\partial f}{\partial \varepsilon_{ij}^{p}}\dot{\varepsilon}_{ij}^{p} = 0. \tag{7}$$

Now, returning to the task of developing an incremental constitutive relation, let

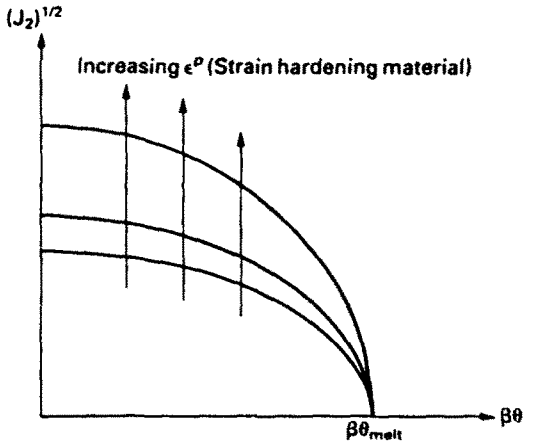

Fig. 2. Expansion of the yield surface ($\theta_{ref} = 0$).

$$q_{ij} = \frac{\partial f}{\partial \sigma_{ij}} \tag{8a}$$

$$p_{ij} = -\frac{\partial f}{\partial \varepsilon^{p}_{ij}} \tag{8b}$$

$$w = \frac{\partial f}{\partial \theta}. \tag{8c}$$

Then, eqns (6) and (7) simplify to

$$\dot{\varepsilon}^{p}_{ij} = \dot{\lambda} q_{ij} \tag{9}$$

$$q_{ij}\dot{\sigma}_{ij} + w\dot{\theta} - p_{ij}\dot{\varepsilon}^{p}_{ij} = 0, \tag{10}$$

respectively. Also, the stresses can be related to the elastic strain ε^{e}_{ij} via the mechanical strain ε^{m}_{ij} and plastic strain ε^{p}_{ij} as:

$$\dot{\sigma}_{ij} = D^{e}_{ijkl}(\dot{\varepsilon}^{m}_{kl} - \dot{\varepsilon}^{p}_{kl}). \tag{11}$$

Substituting (11) into (10) produces

$$q_{ij} D^{e}_{ijkl}(\dot{\varepsilon}^{m}_{kl} - \dot{\varepsilon}^{p}_{kl}) + w\dot{\theta} - p_{ij}\dot{\varepsilon}^{p}_{ij} = 0. \tag{12}$$

After using (9) in (12) and grouping terms, the following relation is obtained for $\dot{\lambda}$:

$$\dot{\lambda} = \frac{q_{ij} D^{e}_{ijkl}\dot{\varepsilon}^{m}_{kl} + w\dot{\theta}}{q_{ij} D^{e}_{ijkl} q_{kl} + q_{ij} p_{ij}}. \tag{13}$$

Next, from (9) and (11)

$$\dot{\sigma}_{ij} = D^{e}_{ijkl}(\dot{\varepsilon}^{m}_{kl} - \dot{\lambda} q_{kl}) \tag{14}$$

and consequently,

$$\dot{\sigma}_{ij} = D^{e}_{ijkl}\dot{\varepsilon}^{m}_{kl} - D^{e}_{ijkl} q_{kl}\left[\frac{q_{mn} D^{e}_{mnrs}\dot{\varepsilon}^{m}_{rs} + w\dot{\theta}}{q_{mn} D^{e}_{mnrs} q_{rs} + q_{mn} p_{mn}}\right]. \tag{15}$$

At this point, the explicit forms of q_{ij}, p_{ij} and w are needed to simplify (15). For the yield function defined by eqn (1), these are, specifically,

$$q_{ij} = s_{ij} \tag{16a}$$

$$p_{ij} = \tfrac{2}{3} H \Gamma \sigma_{ij} \tag{16b}$$

$$w = \frac{2\sigma_y^2}{3}\frac{\theta}{\theta^2_{\text{melt}}}, \tag{16c}$$

where H is the current slope of the uniaxial stress–plastic strain curve. Utilizing (16) and some algebraic manipulation, eqn (15) can be transformed into

$$\dot{\sigma}_{ij} = D^{\text{tep}}_{ijkl}\dot{\varepsilon}^{m}_{kl} - \beta^{\text{tep}}_{ij}\dot{\theta} \tag{17}$$

in which

$$D^{tcp}_{ijkl} = D^{e}_{ijkl} - 2\mu\left[\frac{3s_{ij}s_{kl}}{2\sigma_y^2\Gamma\left(1+\dfrac{\Gamma H}{3\mu}\right)}\right] \tag{18a}$$

$$\beta^{tcp}_{ij} = \frac{s_{ij}\theta}{\theta^2_{melt}\Gamma\left(1+\dfrac{\Gamma H}{3\mu}\right)}. \tag{18b}$$

This is the desired incremental constitutive relation for the present thermoplastic theory. The above equations together with the modified loading and unloading criteria (Boley and Weiner, 1960) provide a suitable first-order thermoplastic model.

3. INTEGRAL FORMULATIONS

In this section, the boundary integral formulation developed previously in Dargush and Banerjee (1989, 1990) for thermoelasticity will be extended to include the effects of plasticity. Basically, the initial stress approach, outlined in Banerjee and Butterfield (1981), is adopted herein. For this approach, the incremental initial stresses are defined as

$$\dot{\sigma}^{0}_{ij} = \dot{\sigma}^{e}_{ij} - \dot{\sigma}_{ij} \tag{19}$$

where

$$\dot{\sigma}^{e}_{ij} = D^{e}_{ijkl}\dot{\varepsilon}_{kl} - \beta^{e}_{ij}\dot{\theta} \tag{20}$$

and $\dot{\sigma}_{ij}$ is given by (17). This relationship between the initial, elastic and total stress rates is illustrated in Fig. 3 for a one-dimensional case. Now, upon writing the incremental equilibrium equation,

$$\dot{\sigma}_{ij,j} = \dot{\sigma}^{e}_{ij,j} - \dot{\sigma}^{0}_{ij,j} = 0, \tag{21}$$

it becomes obvious that the term $-\dot{\sigma}^{0}_{ij,j}$ can be treated as an incremental body force. As a result, the integral equation, developed from (21) and the appropriate reciprocal theorem of Ionescu-Cazimir (1964), will contain volume integrals due to the appearance of these

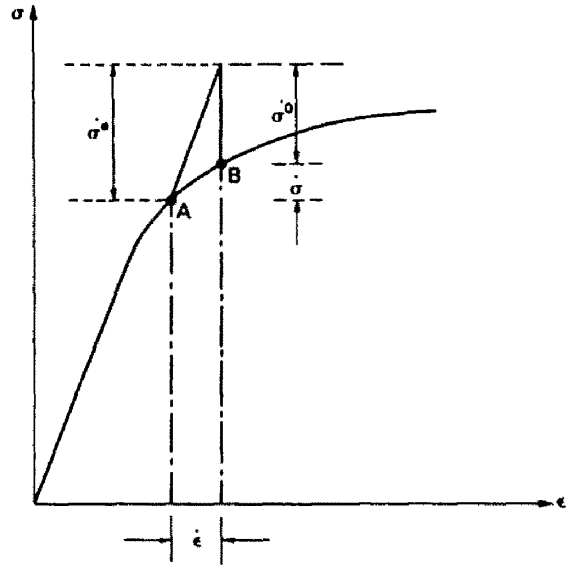

Fig. 3. Initial stress definition.

initial stresses. In addition, heat is generated through inelastic dissipation and must be accounted for in the energy balance. This leads to the requirement for a body source in the differential energy equation and another volume term in the integral formulation. The resulting extension of the boundary integral equation of Dargush and Banerjee (1989, 1990) can be written in incremental form as

$$c_{\beta\alpha}(\xi)\dot{u}_\beta(\xi,t) = \int_S [\dot{G}_{\beta\alpha} * t_\beta(X,t) - \dot{F}_{\beta\alpha} * u_\beta(X,t)]\,dS(X) + \int_V [\dot{Q}_{ik\alpha} * \dot{\sigma}^0_{ik}(Z,t) + \dot{G}_{\theta\alpha} * \dot{\psi}^0(Z,t)]\,dV(Z), \quad (22)$$

where the heat sources are

$$\psi^0(Z,t) = \gamma \sigma_{ij} \dot{\varepsilon}^p_{ij} \quad (23)$$

with γ as a dimensionless material parameter specifying the portion of the inelastic dissipation converted into heat. In eqn (22) and for the remainder of this paper, Latin indices vary from one to three. Greek indices range from one to four, except for the subscript θ which assumes only the value of four. Furthermore, in three dimensions

$$u_\beta = \{u_1 \quad u_2 \quad u_3 \quad \theta\} \quad (24a)$$

$$t_\beta = \{t_1 \quad t_2 \quad t_3 \quad q\} \quad (24b)$$

where t_i is the surface traction vector and q is the normal heat flux. The kernel $Q_{ik\alpha}$, appearing in (22), can be derived from $G_{i\alpha}$ via

$$Q_{ik\alpha} = \frac{1}{2}\left(\frac{\partial G_{i\alpha}}{\partial X_k} + \frac{\partial G_{k\alpha}}{\partial X_i}\right). \quad (25)$$

All of the kernels appearing in (22) are defined explicitly in the Appendix for three-dimensional bodies. This definition is consistent with the form of (22). Previously, in Dargush and Banerjee (1990), the kernel functions were inadvertently transposed.

A closer examination of the Appendix reveals that all kernels can be decomposed into steady-state and transient components, with the former containing singularities and the latter remaining non-singular. This characteristic was discussed in Dargush and Banerjee (1989, 1990) for the boundary kernels $G_{\beta\alpha}$ and $F_{\beta\alpha}$. Since a derivative of $G_{i\alpha}$ is involved in forming $Q_{ik\alpha}$, the singularity in ${}^*Q_{ik\alpha}$ has the same order as that in ${}^*F_{\beta\alpha}$. However, ${}^*Q_{i\beta}$ appears within a volume integral, whereas ${}^*F_{\beta\alpha}$ is associated with a surface integral. This increased dimensionality reduces the severitiy of the integration of ${}^*Q_{ik\alpha}$ to the weakly singular variety. Therefore, numerical quadrature will be suitable for the evaluation of the domain integrals appearing in (22).

Next, notice that a considerable degree of coupling is embodied in eqn (22). In particular, the inelastic dissipation produces deformation along with the expected thermal response. This coupling can be quite significant in practical problems. For example, whenever plastic flow occurs in the metal, heat is generated via inelastic dissipation, thus elevating the temperature locally. The resulting thermal gradients can combine, with a reduction in yield strength due to thermal dilatation, to produce further plastic flow. In many instances, this contribution of the inelastic dissipation must be included in the formulation to properly monitor the movement of the plastic front and to determine residual stresses. Clearly, in these cases, a coupled formulation, involving the simultaneous consideration of equilibrium and energy balance, is mandatory.

In thermoplasticity, the integral formulation explicitly involves initial stress and heat source rates, which are not known *a priori*. Thus, eqn (22) alone is not sufficient to solve

the thermoplastic problem. In general, the initial stress rates appearing in (22) must be calculated from (19) through an iterative process. This, in turn, requires the evaluation of the total stress rates $\dot{\sigma}_{ij}$. Therefore, unlike the thermoelastic problem, the determination of interior and boundary stress is no longer optional, but rather compulsory.

With that in mind, an integral expression for $\dot{\sigma}_{ij}$ can be derived directly from (22). For points ξ, not on the surface of the body

$$\dot{\sigma}_{ij}(\xi,t)=\int_S [\dot{E}_{\beta ij}*\dot{t}_\beta(X,t)-\dot{D}_{\beta ij}*\dot{u}_\beta(X,t)]\,\mathrm{d}S(X)$$
$$+\int_V [\dot{P}_{klij}*\dot{\sigma}^0_{kl}(Z,t)]\,\mathrm{d}V(Z)+J_{klij}\dot{\sigma}^0_{kl}(\xi,t)+\int_0 [\dot{E}_{\theta ij}*\psi^0(Z,t)]\,\mathrm{d}V(z) \quad (26)$$

where $E_{\beta ij}$, P_{klij} and J_{klij} are all defined in the Appendix.

The first volume integral, appearing in (26), must be evaluated over $V-V_\varepsilon$ as $V_\varepsilon\to 0$, where V_ε is a spherical exclusion centered about ξ. This is required due to the strongly singular nature of the P_{klij} kernel. The term J_{klij} results from the analytical integration of P_{klij} over V_ε for a locally-homogeneous stress distribution. Since the singularity of the P_{klij} kernel is identical to that present in the corresponding static plasticity stress kernel, J_{klij} is equivalent to the standard plasticity jump terms (Banerjee and Raveendra, 1986).

However, for points ξ on the boundary, eqn (26) is no longer suitable due to the strong singularities in the surface integrals. Thus, for boundary stresses, an alternate procedure, similar to that outlined in Banerjee and Raveendra (1986) and Dargush and Banerjee (1989), is utilized. The procedure involves the following relations,

$$\dot{\sigma}_{ij}(\xi,t)n_j(\xi)=\dot{t}_i(\xi,t) \quad (27a)$$

$$\dot{\sigma}_{ij}(\xi,t)=\frac{D^e_{ijkl}}{2}[\dot{u}_{k,l}(\xi,t)+\dot{u}_{l,k}(\xi,t)]-\beta\delta_{ij}\dot{u}_\theta(\xi,t)-\dot{\sigma}^0_{ij}(\xi,t) \quad (27b)$$

$$\frac{\partial x_l}{\partial\zeta}\dot{u}_{i,l}(\xi,t)=\frac{\partial\dot{u}_i(\xi,t)}{\partial\zeta} \quad (27c)$$

in which ζ represents the local coordinate system constructed on the surface at ξ. Equations (27) can now be solved for $\dot{\sigma}_{ij}$ in terms of the incremental traction, displacements and initial stresses without the need for temporal or spatial integration.

The integral expressions (22) and (26), along with relationships (27), provide the foundation for the present boundary element method for thermoplasticity. In the next section, the numerical implementation of this new boundary element formulation is discussed.

4. NUMERICAL IMPLEMENTATION

4.1. *Introduction*

Most of the techniques discussed in Dargush and Banerjee (1989, 1990) for thermoelastic implementation remain valid for thermoplasticity. Consequently, in the current section, only the items that differ substantially from those outlined previously will be detailed. In the first subsection, some notational changes are introduced in an otherwise identical, temporal discretization. These changes are the result of the incremental, rather than total, formulation. Then, the following two subsections pertain to the domain discretization and integration, respectively. The corresponding surface operations were described adequately in the aforementioned references. Assembly also remains as before, except that matrices associated with the volume integrals must be collocated and stored. However, the strategy of solution is quite different. Thus, the final subsection details the iterative algorithm employed for the solution of the thermoplastic problem. This entire

implementation was accomplished within the general purpose boundary element program GPBEST.

4.2. *Temporal discretization*

For the temporal discretization, the time axis is subdivided into N equal increments. Within each increment, the field variables are assumed constant. However, now, in the thermoplastic formulation, these field variables are incremental quantities. This poses no particular problem, therefore, following the temporal approximation, the integral equations (22) and (26) can be written

$$c_{\beta\alpha}(\xi)\Delta u_\beta^N(\xi) = \sum_{n=1}^{N} \left\{ \int_S [G_{\beta\alpha}^{N+1-n}(X-\xi)\Delta t_\beta^n(X) - F_{\beta\alpha}^{N+1-n}(X-\xi)\Delta u_\beta^n(X)]\,dS(X) + \int_V [Q_{ik\alpha}^{N+1-n}(Z-\xi)\Delta\sigma_{ik}^{0n}(Z) + G_{i\alpha}^{N+1-n}(Z-\xi)\Delta\psi^{0n}(Z)]\,dV(Z) \right\} \quad (28a)$$

$$\Delta\sigma_{ij}^N(\xi) = \sum_{n=1}^{N} \left\{ \int_S [E_{\beta ij}^{N+1-n}(X-\xi)\Delta t_\beta^n(X) - D_{\beta ij}^{N+1-n}(X-\xi)\Delta u_\beta^n(X)]\,dS(X) + \int_V [P_{klij}^{N+1-n}(Z-\xi)\Delta\sigma_{kl}^{0n}(Z) + E_{0ij}^{N+1-n}(Z-\xi)\Delta\psi^{0n}(Z)]\,dV(Z) \right\} + J_{klij}\Delta\sigma_{kl}^{0N}(\xi). \quad (28b)$$

Notice that in (28), the rate form of the field variables that appeared in (22) and (26) has been replaced, appropriately, by an incremental form. This is consistent with the temporal approximation of constant field variables within each time increment. Also, note that the superscript ^{0} represents an initial stress or initial heat source while ^{n} refers to the time increment index. Occasionally, in the following, ^{n} will assume a specific integer value; however, in all cases where both are used, the ^{0} will appear first to avoid confusion.

4.3. *Spatial discretization*

The surface discretization proceeds exactly as for thermoelasticity by subdividing the boundary into elements defined by nodal points and shape functions. In thermoplasticity, since volume integrals appear in eqns (28), the domain must also be modeled. However, this domain discretization can be restricted to the regions in which plasticity occurs. In many practical problems, this plastic region may amount to only a small percentage of the total body. The remainder of the volume is thermoelastic. Consequently, initial stresses and heat sources in these regions are zero, and the volume integrals vanish, thereby eliminating the need for any discretization. This constitutes a significant advantage over domain-based approaches, such as the finite element method.

For the regions in which plasticity is expected, the volume is subdivided into cells. The geometry of each cell is again defined by nodal points and quadratic shape functions. A 20-noded solid cell is used. The quadratic geometric variation permits the representation of intricate shapes with a minimal number of cells. Meanwhile, either a linear or quadratic variation can be employed for the functional representation. Formally, then, for any cell,

$$Z(\zeta) = z_i(\zeta) = M_w(\zeta)z_{iw} \quad (29)$$

$$\Delta\sigma_{ij}^{0n}(\zeta) = M_\omega(\zeta)\Delta\sigma_{ij\omega}^{0n} \quad (30a)$$

$$\Delta\psi^{0n}(\zeta) = M_\omega(\zeta)\Delta\psi_\omega^{0n} \quad (30b)$$

where

ζ intrinsic coordinates
M_w, M_ω shape functions
z_{iw} nodal coordinates of cell

$\Delta\sigma_{ij\omega}^{0n}$ nodal values of incremental initial stess
$\Delta\psi_{\omega}^{0n}$ nodal value of incremental initial heat source.

In the above, the index w varies from one to the number of geometric nodes, while ω ranges from one to the number of functional nodes in the cell under consideration. It should be emphasized that only the incremental initial stress and heat source are represented by these shape functions. The variation of incremental displacement and temperature is not at all restricted within the cell. Consequently, steep temperature gradients, that develop near the surface due to sudden thermal loading, can still be captured without the need for an excessive number of cells. On the other hand, the finite element method often requires an extremely fine mesh to properly represent the severe gradients.

With the above spatial discretization in mind, the integral equations can now be rewritten. For the incremental generalized displacement this becomes

$$\begin{aligned} c_{\beta\alpha}(\xi)\Delta u_{\beta}^{N}(\xi) = \sum_{n=1}^{N}\Bigg\{\sum_{m=1}^{M}\Bigg[&\Delta t_{\beta\omega}^{n}\int_{S_m} G_{\beta\alpha}^{N+1-n}(X(\zeta)-\xi)N_{\omega}(\zeta)\,\mathrm{d}S(X(\zeta)) \\ &-\Delta u_{\beta\omega}^{n}\int_{S_m} F_{\beta\alpha}^{N+1-n}(X(\zeta)-\xi)N_{\omega}(\zeta)\,\mathrm{d}S(X(\zeta))\Bigg] \\ &+\sum_{m=1}^{L}\Bigg[\Delta\sigma_{ik\omega}^{0n}\int_{V_m} Q_{ik\alpha}^{N+1-n}(Z(\zeta)-\xi)M_{\omega}(\zeta)\,\mathrm{d}V(Z(\zeta)) \\ &+\Delta\psi_{\omega}^{0n}\int_{V_m} G_{0\alpha}^{N+1-n}(Z(\zeta)-\xi)M_{\omega}(\zeta)\,\mathrm{d}V(Z(\zeta))\Bigg]\Bigg\} \end{aligned} \tag{31a}$$

where

$$V=\sum_{m=1}^{L} V_m$$

and L is the number of volume cells. A similar transformation occurs for the incremental stress eqn (28b), producing

$$\begin{aligned} \Delta\sigma_{ij}^{N}(\xi) = \sum_{n=1}^{N}\Bigg\{\sum_{m=1}^{M}\Bigg[&\Delta t_{\beta\omega}^{n}\int_{S_m} E_{\beta ij}(X(\zeta)-\xi)N_{\omega}(\zeta)\,\mathrm{d}S(X(\zeta)) \\ &-\Delta u_{\beta\omega}^{n}\int_{S_m} D_{\beta ij}(X(\zeta)-\xi)N_{\omega}(\zeta)\,\mathrm{d}S(X(\zeta))\Bigg] \\ &+\sum_{m=1}^{L}\Bigg[\Delta\sigma_{kl\omega}^{0n}\int_{V_m} P_{klij}^{N+1-n}(Z(\zeta)-\xi)M_{\omega}(\zeta)\,\mathrm{d}V(Z(\zeta)) \\ &+\Delta\psi_{\omega}^{0n}\int_{V_m} E_{0ij}^{N+1-n}(Z(\zeta)-\xi)M_{\omega}(\zeta)\,\mathrm{d}V(Z(\zeta))\Bigg]\Bigg\} \\ &+J_{klij}\Delta\sigma_{kl}^{0N}(\xi). \end{aligned} \tag{31b}$$

In these equations, M is the total number of boundary elements, while $\Delta t_{\beta\omega}^{n}$ and $\Delta u_{\beta\omega}^{n}$ are the generalized incremental nodal tractions and displacements, respectively. Furthermore, $N_{\omega}(\zeta)$ is the shape function defining the variation of Δt_{β}^{n} and Δu_{β}^{n} within an element.

4.4. *Numerical integration*

The integration techniques required for the evaluation of the surface integrals appearing in (31) have been extensively discussed in Dargush and Banerjee (1989, 1990). Thus, in this subsection, only the volume integrals will be discussed. Recall, from eqn (26), that the strong singularity in the domain integral involving the P_{klij} kernel was removed via analytical

integration. [The result of this analytical integration is the J_{kli} jump term in eqn (31b)]. Consequently, all of the remaining volume integrals are, at worst, only weakly singular, and Gaussian quadrature is appropriate. As with the surface integration techniques, sub-segmentation and variable quadrature order are used to control error. Separate schemes are employed for singular and non-singular cases. Specific details of this volume integration algorithm which is identical to the ordinary elastoplastic case can be found in Mustoe (1984) and Banerjee and Raveendra (1986).

4.5. *Solution algorithm*

The assembly process proceeds as in the thermoelastic case, except that an additional collocation is required for the volume nodes. Therefore, after assembly, the following two sets of algebraic equations are produced, based upon (31a) and (31b), respectively:

$$[A^1]\{\Delta x^N\} = [B^1]\{\Delta y^N\} - [Q^1]\{\Delta\sigma^{0N}\} - [G_a^1]\{\Delta\psi^{0N}\} + \{R^N\} \tag{32a}$$

$$\{\Delta\sigma^N\} = -[E^1]\{\Delta t^N\} + [D^1]\{\Delta u^N\} - [P^1]\{\Delta\sigma^{0N}\} - [E_a^1]\{\Delta\psi^{0N}\} + \{R_\sigma^N\} \tag{32b}$$

where

$$\{R^N\} = -\sum_{n=1}^{N-1}([G^{N+1-n}]\{\Delta t^n\} - [F^{N+1-n}]\{\Delta u^n\} + [Q^{N+1-n}]\{\Delta\sigma^{0n}\} + [G_a^{N+1-n}]\{\Delta\psi^{0n}\}) \tag{33a}$$

$$\{R_\sigma^N\} = -\sum_{n=1}^{N-1}([E^{N+1-n}]\{\Delta t^n\} - [D^{N+1-n}]\{\Delta u^n\} + [P^{N+1-n}]\{\Delta\sigma^{0n}\} + [E_a^{N+1-n}]\{\Delta\psi^{0n}\}), \tag{33b}$$

represent the effect of past events. In these questions, all of the matrices correspond to kernels present in (31), except for $[A^1]$ and $[B^1]$ which are formed from $[F^1]$ and $[G^1]$. The matrix $[P^1]$ contains the contributions of the jump terms J_{kli} along with results of the volume integration of the P_{kli}^l kernel. Additionally,

$\{\Delta x^N\}$ unknown components of $\{\Delta u^N\}$ and $\{\Delta t^N\}$

$\{\Delta y^N\}$ known components of $\{\Delta u^N\}$ and $\{\Delta t^N\}$.

At first glance, it may appear that a prodigious amount of work is required to form $\{R^N\}$ and $\{R_\sigma^N\}$ at each time step. However, such is not the case because of the nature of the thermoelastic fundamental solutions which form the basis of all of the kernel functions. In fact, only a small portion of $[G^n]$, $[F^n]$, $[E^n]$ and $[D^n]$ is time dependent. The remaining terms vanish from (33), as do the entire $[Q^n]$ and $[P^n]$ contribution. As a result, eqns (33) simplify to the following:

$$\{R^N\} = -\sum_{n=1}^{N-1}([G_a^{N+1-n}]\{\Delta q^n\} - [F_a^{N+1-n}]\{\Delta\theta^n\} + [G_a^{N+1-n}]\{\Delta\psi^{0n}\}) \tag{34a}$$

$$\{R_\sigma^N\} = -\sum_{n=1}^{N-1}([E_a^{N+1-n}]\{\Delta q^n\} - [D_a^{N+1-n}]\{\Delta\theta^n\} + [E_a^{N+1-n}]\{\Delta\psi^{0n}\}). \tag{34b}$$

Thus, convolution is only required for the flux, temperature and body source contributions, and the entire boundary element formulation becomes extremely attractive for thermoplastic analyses.

The solution of (32) requires the complete knowledge of the incremental initial stresses and heat sources in the plastic region. Since these items are not known *a priori*, an iterative

scheme must be introduced. In the present work, an algorithm, developed originally by Ahmad and Banerjee (1990) for transient dynamic plasticity, is employed.

It should be noted that in this iterative scheme, the non-linearities enter the formulation entirely through the right-hand side contributions from the initial stresses and body heat sources. As a result, the system matrix $[A^{-1}]$, which must be decomposed, remains identical to that used in the comparable boundary-only thermoelastic analysis.

The algorithm can also provide solutions for steady-state thermoplasticity. In such problems, time becomes strictly a pseudo quantity. Consequently, the inelastic dissipation effects vanish, the kernels simplify considerably, and convolutions are no longer required. Since, in practical terms, steady-state thermoplasticity is an important subset of the general theory, a streamlined algorithm for this static problem has been included in the numerical implementation.

5. APPLICATIONS

5.1. *Slow heating of an aluminum block*

As a first demonstration example, the slow heating of a partially restrained aluminum block is considered. A 1 in. × 1 in. × 1 in. block, resting stress free at 0 F, is constrained against lateral deformation in the X and Z directions, but permitted to elongate freely in the Y direction. The face at $Y = 1.0$ in. is elevated very slowly to a final temperature of 200 F, while the remaining five faces are insulated. For this example, it is assumed that the rate of heat input is such that the steady-state thermoplastic formulation applies.

The following standard thermoelastic material properties for aluminum are utilized:

$$E = 10 \times 10^6 \text{ psi}, \qquad \nu = 0.33,$$

$$\alpha = 13 \times 10^{-6} \text{ F}^{-1},$$

$$k = 25 \text{ in.} - \text{lb. (s in. F)}^{-1}, \quad \rho c_e = 200 \text{ in.} - \text{lb. (in.}^3 \text{ F)}^{-1}.$$

In addition, to obtain the thermoplastic response, the aluminum is modeled as a temperature-independent von Mises material with isotropic hardening. A yield stress of 10,000 psi is specified, along with a constant hardening modulus of 2×10^6 psi representing the slope of the uniaxial stress–plastic strain curve.

A simple six-element, 20-node boundary element mesh is employed along with a single 20-node volume cell. A steady-state analysis is then performed with GPBEST at five distinct temperatures ranging from 100 to 200 F. In addition, for comparative purposes, this same problem is examined using BEST3D, the three-dimensional boundary element code developed for NASA (Wilson *et al.*, 1984, 1986). In BEST3D, the temperatures throughout the body must be specified *a priori*. These temperatures are then included as body forces in the volume integrals.

From Figs 4 and 5, it is evident that GPBEST precisely reproduces the deformations and stresses obtained from BEST3D, thus validating the present thermoplastic formulation. Notice that in these figures, the thermoelastic solution is also plotted for reference. Of course, with thermoplastic effects included, increased elongations and greatly reduced confining stresses result.

5.2. *Sudden heating of an aluminum block*

Next, the same aluminum block is investigated under quasistatic conditions. In the present problem, with the block initially at zero temperature, the face at $Y = 1.0$ in. is suddenly raised to 200 F. This, of course, triggers a transient heat conduction process. Thus, the full time-dependent thermoplastic algorithm is utilized. The remainder of the boundary conditions, along with the material properties and boundary element model, are identical to those prescribed in the previous problem.

Once again in addition to the GPBEST analysis, the problem was examined with BEST3D. In the latter instance, exact temperatures, based upon the solution defined in Carslaw and Jaeger (1947), were input for each nodal point. Figure 6 displays the total

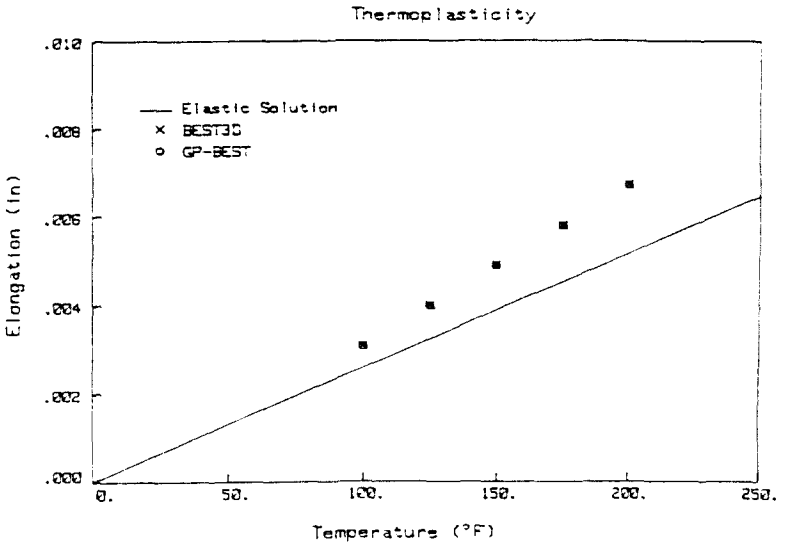

Fig. 4. Slow heating of an aluminium block—elongation.

elongation of the block as a function of time. Slight deviations occur during the first few times steps due primarily to inaccuracies in modeling the early stages of this sudden thermal diffusion process. [See Dargush and Banerjee (1991) for a full discussion of this difficulty.] In general, however, the correlation is good. As expected,the correlation of confining stress is not quite as good. From Fig. 7, obviously considerable deviation is present during the initial few seconds. Afterwards, as the GPBEST temperature profile approaches the exact solution, the stresses from GPBEST and BEST3D correspond within a few per cent. If more accuracy is desired in the early stages of the process, additional mesh and time step refinement is in order.

5.3. *Residual stress in a steel cylinder*

The final example involves determination of the residual stresses resulting from the rapid cooling of a long, 2.5 in. diameter steel cylinder. This cylinder is initially in a stress-free state at 1250 F, and then suddenly exposed to an 80 F fluid. A film coefficient of $h = 12.25$ in.$-$lb. (s in.^{2} F)$^{-1}$ is specified on the cylindrical surface for the ensuing convective process.

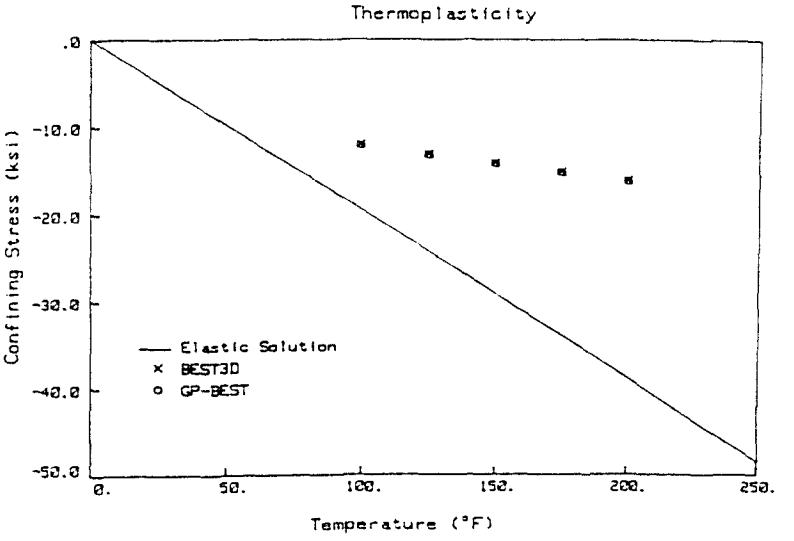

Fig. 5. Slow heating of an aluminium block—confining stress.

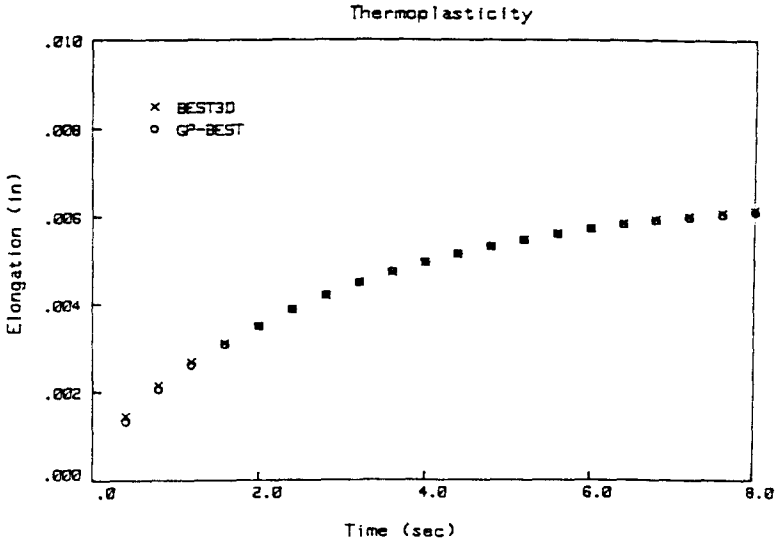

Fig. 6. Sudden heating of an aluminium block—elongation.

The following standard thermoelastic material properties are employed for 1060 steel:

$$E = 30 \times 10^6 \text{ psi}, \qquad \nu = 0.30,$$

$$\alpha = 6 \times 10^{-6} \text{ °F}^{-1},$$

$$k = 5.8 \text{ in.} - \text{lb. (s in. °F)}^{-1}, \quad \rho c_\varepsilon = 283 \text{ in.} - \text{lb. (in.}^3 \text{ °F)}^{-1}.$$

Additionally, a temperature-dependent thermoplastic constitutive model is adopted. In particular, the definitions in eqns (1) and (4) apply, with $\sigma_y = 48$ ksi and $\theta_{\text{melt}} = 1300$ °F. Zero hardening is assumed.

The boundary element surface model, displayed in Fig. 8, consists of 38 source points and 12 elements, while the complete description of the interior requires one extra node and three volume cells. After some numerical experimentation, a time step of 4 s was selected.

Figure 9 shows the temperature response as a function of time for the surface ($r = 1.25$ in.) and center ($r = 0$) of the cylinder at mid-height. Meanwhile, axial stresses at those same

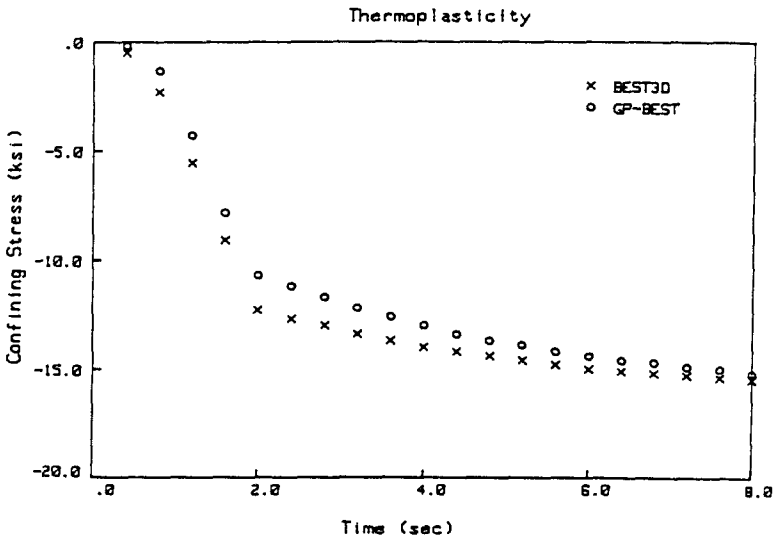

Fig. 7. Sudden heating of an aluminium block—confining stress.

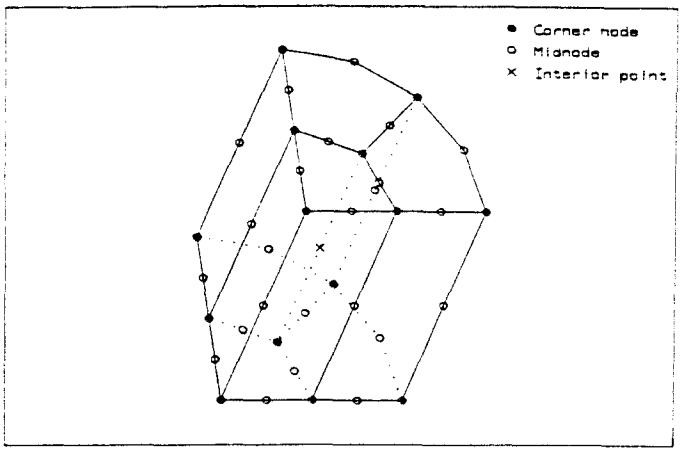

Fig. 8. Residual stress in a steel cylinder—boundary element model.

locations are traced in Fig. 10. Notice that rapid cooling of the surface occurs during the first few seconds. This produces tensile stress in the outer portions and compression toward the center. However, throughout this initial period, the material remains quite hot, and consequently, has a relatively low yield. As a result, significant plastic deformation occurs.

After the beginning 10 s, the yield stress is elevated considerably and the all important thermal gradients diminish, so that no further plastic flow takes place. Instead, elastic unloading commences. At about the 40 s mark, the axial stresses change signs. Thus, the outer fibers go into compressions, while tension occurs in the central portion. This trend continues to steady-state, although for the present analysis, the problem was terminated after the cylinder cooled for 80 s. At that time, the axial stress on the surface and at the center are -20.5 and $+21.1$ ksi, respectively. Of course, the magnitudes of the residual stresses at steady state would be slightly higher.

6. CONCLUSIONS

A new boundary element method was developed for quasistatic problems of thermoplasticity. Naturally, with the introduction of nonlinearities, the integral equations can no longer be formulated strictly in terms of boundary quantities. Volume discretization is

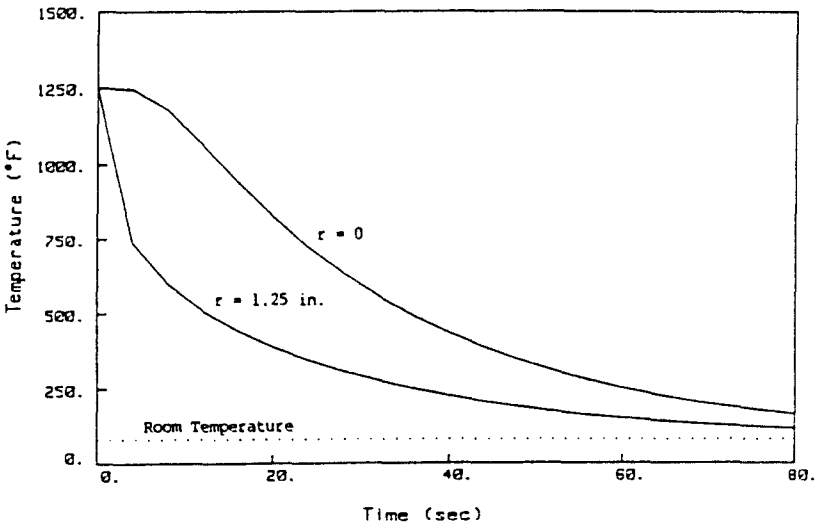

Fig. 9. Residual stress in a steel cylinder—GPBEST temperature results.

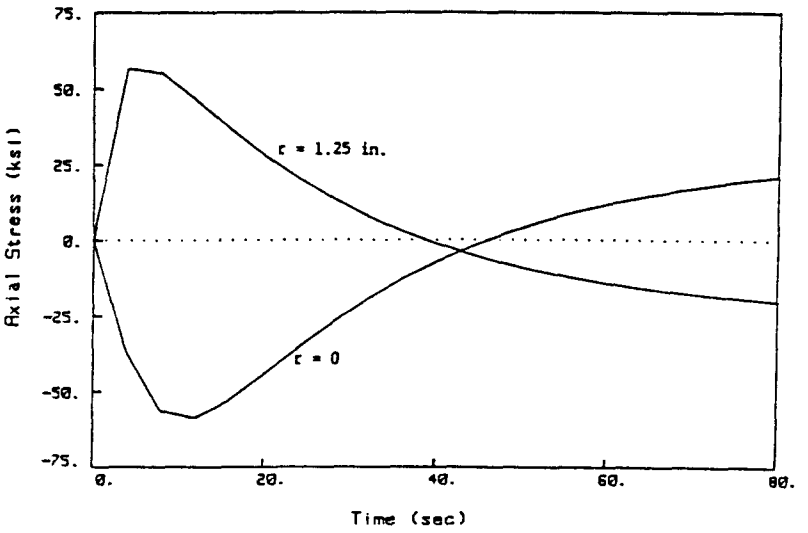

Fig. 10. Residual stress in a steel cylinder—GPBEST axial stress results.

required, but only in the plastic regions. Often, this nonlinearity may be confined to a small portion of the body. For those cases in particular, the BEM is an attractive alternative to finite elements.

A thermally-sensitive von Mises plasticity model with isotropic hardening was derived for use in the BEM. While this constitutive model contains some important features of metal plasticity, it is primarily intended for the purpose of demonstration. In future work, the model will be replaced by more sophisticated versions which include multi-surface kinematic hardening and time-dependent phenomena (i.e. creep) at elevated temperatures. It should be emphasized, however, that even with enhanced material models, the integral formulation and kernel functions, which are presented herein, will remain intact.

Details of the numerical implementation have also been provided. Significant improvements are still needed, however, in the iterative schemes in order to produce a general-purpose engineering analysis tool. Finally, several numerical examples were presented to demonstrate the validitiy of this thermoplastic BEM formulation, and, hopefully, to create interest in its continued development.

REFERENCES

Ahamd, S. and Banerjee, P. K. (1990). Inelastic transient dynamic analysis of three dimensional problems by BEM. *Int. J. Num. Meth. Engng* **29**, 371–390.

Banerjee, P. K. and Butterfield, R. (1981). *Boundary Element Methods in Engineering Science*. McGraw-Hill, London.

Banerjee, P. K., Henry, D. P. and Raveendra, S. T. (1989). Advanced inelastic analysis of solids by the boundary element method. *Int. J. Mech. Sci.* **31**(4), 309–322.

Banerjee, P. K. and Raveendra, S. T. (1986). Advanced boundary element of two- and three-dimensional problems of elastoplasticity. *Int. J. Num. Meth. Engng* **23**, 985–1002.

Banerjee, P. K., Wilson, R. B. and Miller, N. (1988). Advanced elastic and inelastic three dimensional analysis of gas turbine engine structures by BEM. *Int. J. Num. Meth. Engng* **26**, 393–411.

Boley, B. A. and Weiner, J. H. (1960). *Theory of Thermal Stresses*. John Wiley, New York.

Carslaw, H. S. and Jaeger, J. C. (1947). *Conduction of Heat in Solids*. Clarendon Press, Oxford.

Dargush, G. F. (1987). Boundary element methods for the analogous problems of thermomechanics and soil consolidation. Ph.D. dissertation, State University of New York at Buffalo.

Dargush, G. F. and Banerjee, P. K. (1989). Development of a boundary element method for time dependent planar thermoelasticity. *Int. J. Solids Structures* **25**(9), 999–1021.

Dargush, G. F. and Banerjee, P. K. (1990). Boundary element methods in three dimensional thermoelasticity. *Int. J. Solids Structures* **26**(2), 199–216.

Dargush, G. F. and Banerjee, P. K. (1991). Application of the boundary element method to transient heat conduction. *Int. J. Num. Meth. Engng*, to appear.

Ionescu-Cazimir, V. (1964). Problem of linear coupled thermoelasticity. Theorems on reciprocity for the dynamic problem of coupled thermoelasticity. I. *Bull. L'acad. Polonaise des Sci., Series des Sciences Techniques* **12**(9), 473–488.

Mustoe, G. G. W. (1984). Advanced integration schemes over boundary elements and volume cells for two- and three-dimensional nonlinear analysis. In *Developments in Boundary Element Methods*—III (Edited by P. K. Banerjee and S. Mukherjee). Applied Science Publishers, Barking.

Roscoe, K. H. and Burland, J. B. (1968). On the generalized stress–strain behavior of wet clay. In *Engineering Plasticity* (Edited by J. Hayman and F. A. Leckie), pp. 535–609. Cambridge University Press.

Wilson, R. B., Bak, M. J., Nakazawa, S. and Banerjee, P. K. (1984). 3-D inelastic analysis methods for hot section components (base program). First annual status report for the period February 1983 to February 1984, NASA Contractor Report 174700.

Wilson, R. B., Bak, M. J., Nakazawa, S. and Banerjee, P. K. (1986). 3-D inelastic analysis methods for hot section components (base program). Second annual status report for the period February 1984 to February 1985, NASA Contractor Report 175060.

APPENDIX: KERNELS FOR THERMOPLASTICITY

This Appendix contains the detailed presentations of all the kernel functions utilized in the three-dimensional formulation, based upon continuous-source and force-fundamental solutions (Dargush, 1987). For the time-dependent problems, the following relationships must be used to determine the proper form of the functions required in the boundary element discretization. That is,

$$G^n_{\alpha\beta}(X-\xi) = G_{\alpha\beta}(X-\xi, n\Delta t) \qquad \text{for} \quad n = 1$$
$$G^n_{\alpha\beta}(X-\xi) = G_{\alpha\beta}(X-\xi, n\Delta t) - G_{\alpha\beta}(X-\xi, (n-1)\Delta t) \qquad \text{for} \quad n > 1,$$

with similar expressions holding for all the remaining kernels. In the specification of these kernels below, the arguments $(X-\xi, t)$ are assumed.

Note that the indices

i, j, k, l vary from 1 to 3
α, β vary from 1 to 4
0 equals 4.

Additionally,

x_i coordinates of integration point
ξ_i coordinates of field point

$$y_i = x_i - \xi_i \quad r^2 = y_i y_i.$$

For the displacement kernel,

$$G_{ij} = \frac{1}{16\pi r}\frac{1}{\mu(1-\nu)}\left[\left(\frac{y_i y_j}{r^2}\right) + (\delta_{ij})(3-4\nu)\right]$$
$$G_{i0} = 0$$
$$G_{0j} = \frac{1}{8\pi}\left(\frac{\beta}{k(\lambda+2\mu)}\right)\left[\left(\frac{y_j}{r}\right) g_4(\eta)\right]$$
$$G_{00} = \frac{1}{4\pi r}\left(\frac{1}{k}\right)[g_5(\eta)]$$

whereas, for the traction kernel

$$F_{ij} = \frac{1}{8\pi r^2}\frac{1}{1-\nu}\left[-\left(\frac{3y_i y_j y_k n_k}{r^3}\right) - \left(\frac{\delta_{ij} y_k n_k + y_i n_j}{r}\right)(1-2\nu) + \left(\frac{y_j n_i}{4}\right)(1-2\nu)\right]$$
$$F_{i0} = 0$$
$$F_{0j} = \frac{1}{8\pi r}\left(\frac{\beta}{\lambda+2\mu}\right)\left[\left(\frac{y_j y_k n_k}{r^2}\right) f_6(\eta) - (n_j) f_7(\eta)\right]$$
$$F_{00} = \frac{1}{4\pi r^2}\left[\left(\frac{y_k n_k}{r}\right) f_8(\eta)\right].$$

In the above,

$$\eta = r/(ct)^{1/2}$$
$$c = k/\rho c_e$$
$$erf(z) = \frac{2}{\sqrt{\pi}}\int_0^z e^{-x^2}\,dx = 1 - erfc(z)$$
$$h_1(\eta) = erf\left(\frac{\eta}{2}\right) - \frac{\eta}{\sqrt{\pi}} e^{-\eta^2/4}$$

$$g_4(\eta) = erfc\left(\frac{\eta}{2}\right) + \frac{2h_1(\eta)}{\eta^2}$$

$$g_5(\eta) = erfc\left(\frac{\eta}{2}\right)$$

$$f_6(\eta) = erfc\left(\frac{\eta}{2}\right) + \frac{6h_1(\eta)}{\eta^2}$$

$$f_7(\eta) = erfc\left(\frac{\eta}{2}\right) + \frac{2h_1(\eta)}{\eta^2}$$

$$f_8 = 1 - h_1(\eta).$$

For the interior stress boundary kernels,

$$E_{\beta ij} = \frac{2\mu\nu}{1-2\nu}\delta_{ij}\frac{\partial G_{\beta l}}{\partial \xi_l} + \mu\left(\frac{\partial G_{\beta i}}{\partial \xi_j} + \frac{\partial G_{\beta j}}{\partial \xi_i}\right) - \beta\delta_{ij}G_{\beta n}$$

$$D_{\beta ij} = \frac{2\mu\nu}{1-2\nu}\delta_{ij}\frac{\partial F_{\beta l}}{\partial \xi_l} + \mu\left(\frac{\partial F_{\beta i}}{\partial \xi_j} + \frac{\partial G_{\beta j}}{\partial \xi_i}\right) - \beta\delta_{ij}G_{\beta n}$$

where

$$\frac{\partial G_{ij}}{\partial \xi_k} = \frac{1}{16\pi r^2}\frac{1}{\mu(1-\nu)}\left[\left(\frac{3y_i y_k y_k}{r^5} - \frac{\delta_{jk}y_i}{r} - \frac{\delta_{ik}y_j}{r}\right) + \left(\frac{\delta_{ij}y_k}{r}\right)(3-4\nu)\right]$$

$$\frac{\partial G_{0j}}{\partial \xi_k} = \frac{1}{8\pi r}\left(\frac{\beta}{k(\lambda+2\mu)}\right)\left[\left(\frac{y_j y_k}{r^2} - \delta_{jk}\right)g_4(\eta) - \left(\frac{y_j y_k}{r^2}\right)\eta g_4'\right]$$

$$\frac{\partial F_{ij}}{\partial \xi_k} = \frac{1}{8\pi r^3}\frac{1}{(1-\nu)}\left[-\left(\frac{15y_i y_j y_k y_l n_l}{r^4} - \frac{3y_i y_j n_k}{r^2} - \frac{3\delta_{jk}y_i y_l n_l}{r^2} - \frac{3\delta_{ij}y_k y_l n_l}{r^2}\right)\right.$$
$$\left. -\left(\frac{3\delta_{ij}y_k y_l n_l}{r^2} - \delta_{ij}n_k + \frac{3y_i y_k n_j}{r^2} - \delta_{jk}n_i + \frac{3y_i y_k n_i}{r^2} - \delta_{jk}n_i\right)(1-2\nu)\right]$$

$$\frac{\partial F_{0j}}{\partial \xi_k} = \frac{1}{8\pi r^2}\left(\frac{\beta}{\lambda+2\mu}\right)\left[\left(\frac{3y_j y_k y_l n_l}{r^5} - \frac{y_j n_k}{r} - \frac{\delta_{jk}y_l n_l}{r}\right)f_6(\eta) - \left(\frac{y_k n_j}{r}\right)f_7(\eta) - \left(\frac{y_j y_k y_l n_l}{r^3}\right)\eta f_6' + \left(\frac{y_k n_j}{r}\right)\eta f_7'\right]$$

and the prime, ', represents a derivative with respect to η. Thus,

$$f_6' = \frac{\partial f_6(\eta)}{\partial \eta}.$$

Additionally, for the volume kernels

$$Q_{ikz} = \frac{1}{2}\left(\frac{\partial G_{iz}}{\partial x_k} + \frac{\partial G_{kz}}{\partial x_i}\right)$$

where

$$\frac{\partial G_{ij}}{\partial x_k} = -\frac{\partial G_{ij}}{\partial \xi_k}$$

$$\frac{\partial G_{i0}}{\partial x_k} = 0,$$

$$P_{kkj} = \frac{2\mu\nu}{1-2\nu}\delta_{ij}\frac{\partial Q_{klm}}{\partial \xi_m} + \mu\left(\frac{\partial Q_{kli}}{\partial \xi_j} + \frac{\partial Q_{klj}}{\partial \xi_i}\right)$$

$$J_{kkij} = -\frac{1}{15(1-\nu)}[(7-5\nu)\delta_{ki}\delta_{jl} + (1-5\nu)\delta_{kl}\delta_{ij}]$$

with

$$\frac{\partial Q_{kli}}{\partial \xi_j} = \frac{1}{2}\left(\frac{\partial^2 G_{ki}}{\partial x_l \partial \xi_j} + \frac{\partial^2 G_{li}}{\partial x_k \partial \xi_j}\right)$$

$$\frac{\partial^2 G_{ij}}{\partial x_l \partial \xi_k} = \frac{1}{16\pi r^3}\frac{1}{\mu(1-\nu)}\left[-15\left(\frac{y_i y_j y_k y_l}{r^4}\right) + 3\left(\frac{y_i y_j \delta_{kl}}{r^2} + \frac{y_j y_k \delta_{il}}{r^2} + \frac{y_k y_i \delta_{jl}}{r^2} + \frac{y_i y_l \delta_{jk}}{r^2} + \frac{y_j y_l \delta_{ik}}{r^2}\right)\right.$$
$$\left. -3(3-4\nu)\left(\frac{y_k y_l \delta_{ij}}{r^2}\right) + (3-4\nu)(\delta_{ij}\delta_{kl}) - (\delta_{jk}\delta_{il} + \delta_{ik}\delta_{jl})\right].$$